Preparation and characterization of $La_{0.8}Cu_{0.2}MnO_{(3\pm\delta)}$ perovskite-type catalyst for methane combustion [①]

HE Fang(何　方), WANG Hua(王　华), DAI Yong-nian(戴永年)

(Faculty of Materials and Metallurgical Engineering,
Kunming University of Science and Technology, Kunming 650093, China)

Abstract: $La_{0.8}Cu_{0.2}MnO_{(3\pm\delta)}$ perovskite-type catalyst for methane combustion prepared through sol-gel process was characterized by X-ray Diffractometry(XRD), X-ray Photoelectron Spectroscopy(XPS) and Scanning Electron Microscopy(SEM). XPS analyses reveal that the surface characteristics of the catalyst are changed. The lattice defects and oxygen vacancies on the catalyst surface are enhanced due to a part of La^{3+} being substituted by Cu^{2+}. Temperature-programmed-desorption(TPD) and temperature-programmed-reduction(TPR) analyses were carried out to study the catalytic behavior. It is found that there are two O_2-desorption peaks at 350 ℃ and 650 ℃ in the TPD pattern, and two CH_4-consumption peaks at 420 ℃ and 750 ℃ in the TPR patterns respectively, which indicates that the two kinds of oxygen species, so-called α and β oxygen, can react with the methane during catalytic combustion process. The catalytic activity tests were performed in a fixed-bed reactor, and the results show that the $T_{1/2}$ at which the conversion of methane attains 50% of $La_{0.8}Cu_{0.2}MnO_{(3\pm\delta)}$ is lower by 55 ℃ than that of $LaMnO_3$. This indicates that the catalytic activity of $La_{0.8}Cu_{0.2}MnO_{(3\pm\delta)}$ is increased with partial substitution of Cu^{2+} for La^{3+}.

Key words: perovskite-type catalyst; methane catalytic combustion; sol-gel; TPD-TPR-MS characterization

CLC number: O 643　　　　　　　　　　**Document code:** A

1 INTRODUCTION

Catalytic combustion is an environmentally-friendly process without pollutant emissions. Typically, NO_x emission can be reduced dramatically, since the combustion temperature is maintained below 1 673 K[1, 2]. Thus, the catalytic combustion technology has been considered one of the promising technologies for reducing hazardous exhaust gases emissions[3]. Catalytic combustion of methane has gained wide attention in recent years in order to limit environment pollution. Perovskites are mixed oxides of general formula $ABO_{(3\pm\delta)}$, where A is usually a lanthanide ion and B is a transition metal ion. Both A and B can be partially substituted, leading to a wide variety of compositions of general formula $A_{1-x}A'_xB_{1-y}B'_yO_{(3\pm\delta)}$, characterized by structural and electronic defects owing to their non-stoichiometry[4, 5]. The metal ion B is considered to be responsible for the catalytic activity in the complete oxidation reactions, while the ion A, especially when being partially substituted with ion A′ of different valences, determines the formation of crystal lattice vacancies and can stabilize unusual oxidation states for B, leading to different catalytic performance[6]. Perovskite-like samples of formula $La_{1-x}Cu_xMnO_{(3\pm\delta)}$ have been reported to be catalytically active for the complete oxidation of CO, HC and NH_3[7]. Also, it is believed that mixed oxides of the perovskite structure are promising methane combustion catalysts substituting noble metal catalysts[8, 9]. In the present work, $La_{0.8}Cu_{0.2}MnO_{(3\pm\delta)}$ (designated as LCMO below) perovskite-like catalyst for methane catalytic combustion was prepared through sol-gel process, and characterized by XRD, XPS and SEM. Furthermore, the catalytic properties of LCMO for methane combustion were investigated by means of TPD and TPR techniques.

2 EXPERIMENTAL

2.1 Catalyst preparation

The active phase, LCMO, was prepared through the so-called sol-gel method by dissolving $La(NO_3)_3 \cdot 6H_2O$, $Cu(NO_3)_2$ and $Mn(NO_3)_2$ in the desired ratios, in distilled water, and adding the nitrates solutions into a mixed solution of EDTA and ethylene glycol. If it was necessary, some ammonia was added in the solution in order to control the pH value. The solvent was evaporated at 70 ℃ until a very viscous gel was formed, then the gel was dried at 120 ℃ in an oven. The dried gel was heated at 300 ℃ for 6 h and calcined

at 850 ℃ for 20 h in air.

2.2　Catalyst characterization

　　XRD analysis of the catalyst was carried out by using a Rigaku-3105 X-ray diffractometer with Cu K_α radiation. The scanning rate was 8(°)/min with scanning scope from 4° to 80°. XPS measurements were conducted using a Perkin Elmer PHI-550 multifunctional electron spectrometer with Mg K_α radiation. The C 1s peak at 285.00 eV due to adventitious carbon was used as an internal reference. Morphology and particle size were determined by means of a Philip XL30 Scanning Electron Microscope(SEM).

2.3　TPD-TPR-MS analysis

　　The temperature programmed desorption (TPD) of the catalyst was carried out on a Quantachrome Instruments. The experiments were performed in flowing He from room temperature to 1 273 K with a heating rate of 15 K/min and a flow rate of 20 cm^3/min. The composition of the outlet gas was monitored by means of a quadrupolar mass spectrometer. The temperature programmed reduction(TPR) of the catalyst was tested in the same apparatus. 5.0% CH_4(volume fraction) in He was fed to the reactor. Other experimental conditions were the same as those of TPD tests.

2.4　Catalytic activity tests

　　The catalytic oxidation of methane was carried out in a fixed-bed quartz tubular reactor at atmospheric pressure. Briefly, a quartz tubular reactor with 600 mm in length and 18 mm in inside diameter, was put into a tubular furnace. 100 mg of the catalyst was placed in the middle part of the reactor between two flocks of quartz wool. The void part of the reactor tube was filled with quartz beads. The temperature of the catalyst bed was monitored by a thermocouple placed in the centre of the catalyst bed. The temperature of the reactor was maintained by an electronic controller. Prior to catalytic tests, the catalyst was activated in flowing air, such as increasing temperature by 10 ℃/min up to 600 ℃, then keeping for 1 h. The activity tests were performed by feeding a mixture composed of 1% CH_4, 5% O_2, and 94% N_2(volume fraction), and increasing temperature by 5 ℃/min form 200 to 900 ℃. The product analysis was conducted using an on-line gas chromatograph provided with a TC detector, using Helium as carrier gas. The conversion was calculated by using the concentration of methane and confirmed by the yields of CO_2 and CO. In order to examine the effect of the partial substitution of Cu^{2+} in A site on the catalytic activity, the catalytic activity of Cu^{2+} substituted catalyst was compared with that of the non-substituted one.

3　RESULTS AND DISCUSSION

3.1　XRD analysis

　　The XRD pattern of LCMO is shown in Fig. 1. The XRD analysis shows the presence of a perfectly pure crystalline perovskitic phase of LCMO. It is worth to point out that, in some cases, the XRD diffraction patterns obtained for LCMO show a couple of additional weak peaks, probably because of the tendency of Cu or Mn to remain stable in different oxidation states. However, high phase purity of perovskite-type catalyst is achieved for LCMO in most cases.
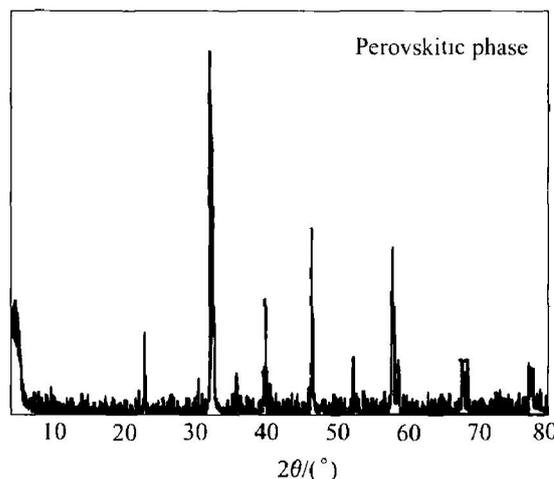

Fig. 1　XRD pattern of $La_{0.8}Cu_{0.2}MnO_{(3\pm\delta)}$ catalyst

3.2　XPS characterization

　　The XPS spectrum of La $3d_{5/2}$ of LCMO is shown in Fig. 2(a). It can be seen that the spectrum is composed of two peaks of La $3d_{5/2}$ binding energy in the catalyst, being at 837.58 and 833.72 eV respectively. Moreover, a satellite peak around each main peak usually can be found during measuring process, which is assigned to the shakeup in the La 3d electrons. It is believed that the shakeup satellite results from the transition of a 3d electron to an empty 4f orbital[10]. The spectrum also indicates that lanthanum ion is the trivalent ion in LCMO. Fig. 2(b) shows the Mn 2p XPS spectrum. The binding energy of Mn 2p is at 653.35 and 642.13 eV. From the results, it seems to be difficult to discern the valence state of manganese ions in LCMO. It is widely believed that the manganese ions co-exist as tri- and quadrivalent in LCMO at the same time, and the amount of Mn^{4+} increases with Cu^{2+} partially substituting B site ions. A typical measure of the skewness is the asymmetry index β used by X-ray spectroscopy. The asymmetry index β= a/b has been defined by Kowalczyk et al[11], in which a is the half-width at half-maximum on the high binding energy side and b is
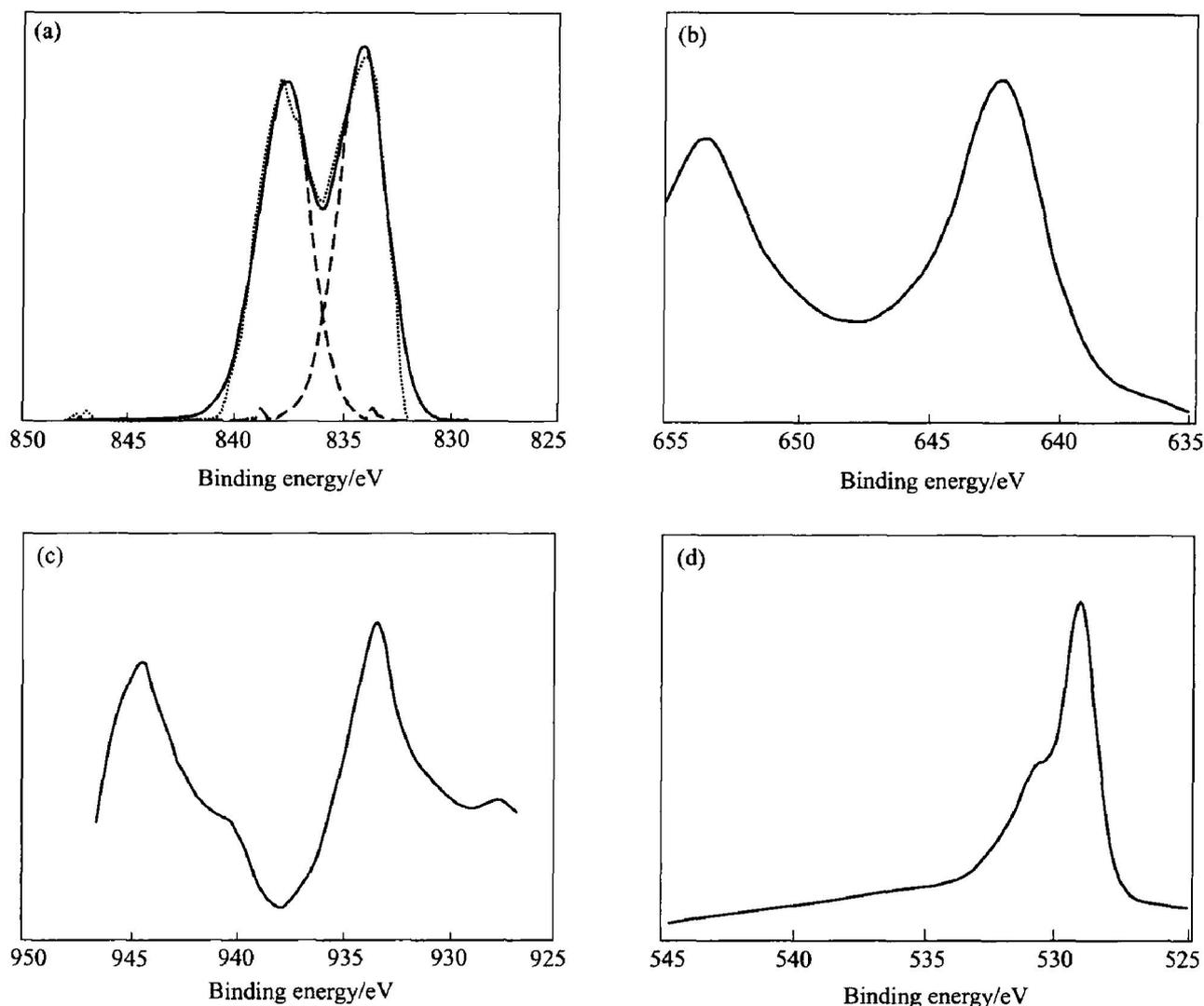
Fig. 2   XPS spectra of La$_{0.8}$Cu$_{0.2}$MnO$_{(3\pm\delta)}$ catalyst
(a) —La 3d$_{5/2}$; (b) —Mn 2p; (c) —Cu 2p$_{3/2}$; (d) —O 1s

the half-width at half-maximum on the low binding energy side. The value of β increases with the increase of x (the molar fraction of Cu) in LCMO, and the Mn^{4+} molar fraction rises with the value of x going up. When x is 0.2 in LCMO, β is measured to be over 1.0, and the shift of peak position shows the change of valence state from Mn^{3+} to Mn^{4+}. Fig. 2(c) shows the spectrum for Cu 2p$_{3/2}$ in the LCMO. There is a weak satellite peak accompanying the main high binding energy peak, which is believed to be the result of the shakeup of Cu 2p in Cu^{2+} because the main peak of Cu^{+} does not have satellite peaks[12]. So, the copper ions in LCMO are mainly composed of Cu^{2+}. Since partial substitution of La^{3+} by Cu^{2+}, according to the condition of electroneutrality condition, the excess negative charge introduced by Cu^{2+}-doping to LCMO is probably compensated either by formation of holes or creation of oxygen vacancies. The oxygen vacancy concentration increases with increasing Cu-doping content. This is beneficial to enhancing the oxygen ionic conductivity, and subsequently im-

proving the catalytic performance of the catalyst. The O 1s XPS spectrum is shown in Fig. 2(d). It can be seen that the spectrum consists of two peaks, which indicates that there are two types of oxygen in LCMO. One type of oxygen with lower binding energy(528.80 eV) is believed as the lattice oxygen. The other type of oxygen with higher binding energy(531.15 eV) corresponds to the absorbed oxygen.

3.3   SEM analysis

SEM micrograph of the LCMO catalysts is presented in Fig. 3. The particle size is about 10 μm. It is noted that the catalyst particles have irregular shape with large porous structure, which, to some extent, increases the surface area of the catalyst.

3.4   O$_2$-TPD and CH$_4$-TPR results

Temperature-programmed desorption (TPD) of oxygen is a powerful technique for the evaluation of catalyst affinity towards oxygen. During
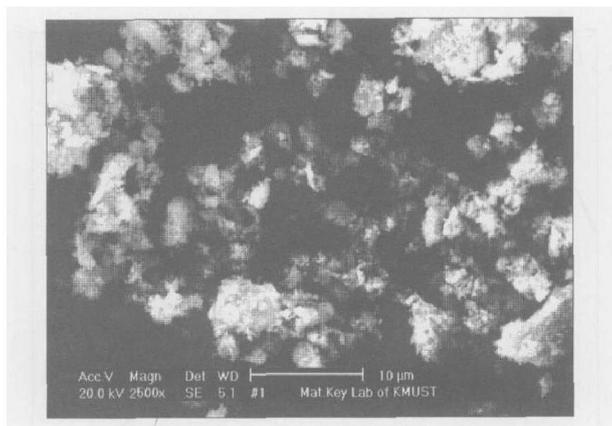
Fig. 3 SEM micrograph of
$La_{0.8}Cu_{0.2}MnO_{(3\pm\delta)}$ catalyst

the TPD analysis of pre-adsorbed oxygen, two desorption peaks, called α and β, can be observed, which are relative to the release of oxygen, adsorbed on the surface or migrating from the bulk, respectively[13]. It is well-known that, when a perovskite is heated in inert atmosphere at high temperature, usually around 800 ℃, oxygen vacancies can form. By cooling in air, these vacancies are filled with adsorbed oxygen and the charge compensation is provided by partial oxidation of the metal B ion. As mentioned above, a TPD analysis of a perovskite-type materials reveals two possible desorption peaks, called α and β, widely reported in Refs. [14, 15]. The α peak, usually observed at lower temperature, represents the desorption of oxygen adsorbed on the catalyst surface and it is not always observable, depending on the concentration of filled oxygen vacancies on the catalyst surface. In particular, its onset temperature and intensity depend partially on the nature of metal B, but mainly on the substitution degree of the A ion with a cation of different valence. The β peak corresponds to the lattice oxygen desorption process. It, characterized by higher onset temperature, strictly depends on the nature of the B ion, and is correlated to its partial reduction to a lower oxidation state. The onset temperature of the β peak is usually very near that of thermal decomposition of the pure B metal oxide. For instance, the onset temperature of the LCMO β peak is near the decomposition temperature of pure Mn_2O_3.

Fig. 4 illustrates the Oxygen TPD-MS pattern for LCMO catalyst. As shown in Fig. 4, there are two peaks in the TPD spectrum of the catalyst which correspond to the above mentioned α and β peaks respectively. LCMO shows an intense α peak around 350 ℃, while the onset temperature of the β peak is approximately 650 ℃, and the maximum of the β desorption peak reaches at around 750 ℃. The appearance of an intense α peak indicates a high concentration oxygen vacancies and defects on

the surface of the catalyst. Thus, it may be concluded that $La_{0.8}Cu_{0.2}MnO_{(3\pm\delta)}$ possesses a high concentration of oxygen vacancies and defects. In comparison, according to the Ref. [13], $LaMnO_{(3\pm\delta)}$ does not show any α desorption peak. This means that it is possible to introduce different defective sites through partially substituting La ion by Cu. Indeed, the partial substitution of Cu for La leads to a change of the intensity and the onset temperature of α peak. The β peak is assigned to the release of the lattice oxygen in the catalyst. The existence of the β peak and its onset temperature can be adopted as a qualitative index to describe the reducibility and oxygen mobility of the catalyst. This peak has been attributed to Mn^{4+} reduction to Mn^{3+} or lower valence state during the oxygen desorption process, where Mn^{4+} is formed by the substitution of Cu^{2+} for La^{3+}. So, Cu-doping can increase the amount of Mn^{4+} in the catalyst, in consequence increasing the area of β peak. As a result, the performance of the catalyst is enhanced to some extent.
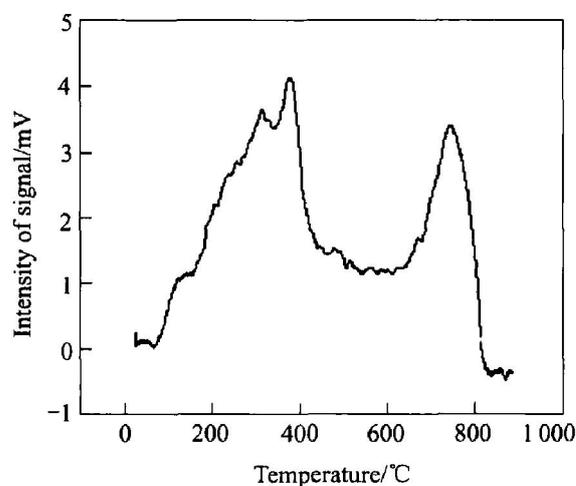

Fig. 4 Oxygen TPD-MS pattern of
$La_{0.8}Cu_{0.2}MnO_{(3\pm\delta)}$ catalyst

The temperature programmed reduction of the catalyst was performed with 5% CH_4 in He from room temperature to 1 000 ℃ with a heating rate of 15 ℃/min and a flow rate of 20 cm^3/min. Fig. 5 shows the CH_4-TPR pattern of $La_{0.8}Cu_{0.2}MnO_{(3\pm\delta)}$ catalyst. Two reduction peaks positioned at approximately 420 and 750 ℃, respectively, are observed for the catalyst. As mentioned above, there are two kinds of oxygen species on the surface of the catalyst, so called α and β oxygen respectively. According to the O_2-TPD analysis, α oxygen is desorbed at relatively lower temperature. So in the TPR pattern, the reduction peak at lower temperature is attributed to the α oxygen. By contrast, the reduction peak at about 750 ℃ may be assigned to the reduction of B site ion to lower valences. In this case, the later peak assigned to the reduction

of Mn^{4+} to Mn^{3+} or Mn^{2+}. With partially Cu-doping in the A site, there are Cu^{2+} ions in the lattice of the catalyst, which may be interacted with the Mn ions and reacted with CH$_4$ during the temperature programmed reduction process[16]. Compared with the TPR profiles of La-Mn-O mixed oxide without Cu-doping, the reduction peaks of LCMO appear at lower temperature. It is probable that Cu-doping in the catalyst can decrease the reaction activation energy between catalyst and CH$_4$ and enhance oxidation activity.
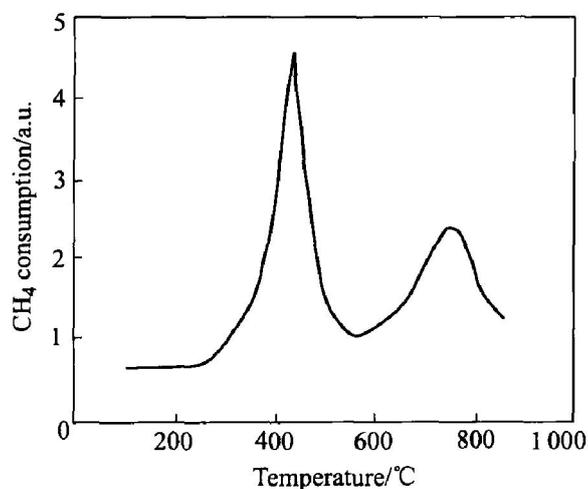

Fig. 5 CH$_4$-TPR pattern of
La$_{0.8}$Cu$_{0.2}$MnO$_{(3\pm\delta)}$ catalyst

3.5 Catalytic activity

The combustion of methane was studied on the La$_{0.8}$Cu$_{0.2}$MnO$_{(3\pm\delta)}$ and LaMnO$_3$ catalyst series over a wide temperature range from 473 K to 1 173 K. Activity data expressed as CH$_4$ conversion ratio are given in Fig. 6 as a function of temperature. Since the CH$_4$ conversion data depicted in Fig. 6 are obtained with the same catalyst mass and specific area varying in a narrow range, it appears more appropriate to reveal the catalyst performance in terms of intrinsic activity. We can see that con-
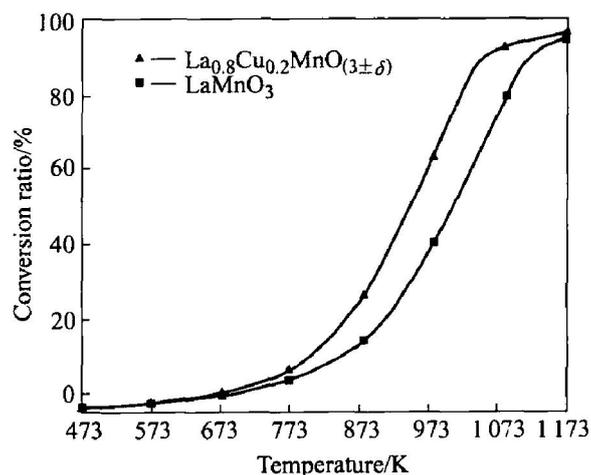
version starts at 573 K for La$_{0.8}$Cu$_{0.2}$MnO$_{(3\pm\delta)}$ and LaMnO$_3$. La$_{0.8}$Cu$_{0.2}$MnO$_{(3\pm\delta)}$ shows a higher catalytic activity than LaMnO$_3$. La$_{0.8}$Cu$_{0.2}$MnO$_{(3\pm\delta)}$ and LaMnO$_3$ show the value of $T_{1/2}$ at about 948 K and 1 003 K respectively ($T_{1/2}$, being the temperature at which the conversion of methane attains 50%, is an important parameter characterizing the activity of catalysts[17]). The temperatures of CH$_4$ full conversion of these two kinds of catalysts are very close. But in general, the Cu^{2+} partially substituted perovskite is more active than LaMnO$_3$.

4 CONCLUSIONS

The LCMO catalyst prepared by sol-gel method is proved to be thermally stable material of high surface area and highly perovskitic crystalline, hence, of high catalytic activity. The XPS analysis results show that with the substitution of Cu for La in the catalyst, Mn^{4+} and the oxygen vacancy concentration increase significantly, meanwhile the catalytic activity for methane combustion increases. The catalytic activity tests confirm these results. There are two kinds of oxygen species, α and β oxygen, on LCMO surface, corresponding to adsorption oxygen with high electron binding energy and lattice oxygen with low electron binding energy. The oxygen species and redox performance of the LCMO oxide were investigated by means of TPD and TPR techniques. There are two peaks both in O$_2$-TPD and CH$_4$-TPR patterns, which means that the two kinds of oxygen species can be involved into the methane combustion reaction. It is possible that in redox mode the lattice oxygen from the LCMO catalyst instead of molecular O$_2$ reacts with methane to the partial or complete oxidation production. The results of catalytic activity tests show that La$_{0.8}$Cu$_{0.2}$MnO$_{(3\pm\delta)}$ exhibits a better catalytic activity for methane combustion than LaMnO$_3$.

Fig. 6 Methane conversion ratio vs temperature of
two kinds of catalyst

REFERENCES

[1] Cho S J, Song K S, Ryu I S, et al. Characteristics of methane combustion over La-Cr-O catalysts [J]. Catalysis Letters, 1999, 58: 63－66.

[2] XU Xiu-feng, PAN Yan-fei, LIU Yan-xia, et al. Catalytic combustion of methane over MnO$_x$/ZrO$_2$-Al$_2$O$_3$ catalysts [J]. Journal of Natural Gas Chemistry, 2003, 12(4): 228－232.

[3] Terrible D, Trovarelli A, de Leitenburg C, et al. Catalytic combustion of hydrocarbons with Mn and Cu doped ceria ± zirconia solid solutions [J]. Catalysis Today, 1999. 47: 133－140.

[4] MA Wen-hui, XIE Gang, CHEN Shu-rong, et al. Solid-state synthesis of Sr- and Co-doped LaMnO$_3$[J]. Trans Nonferrous Met Soc China, 2001, 11(6): 904－907.

[5] Leanza R, Rossetti I, Fabbrini L, et al. Perovskite ca-

talysits for the catalytic flameless combustion of methane preparation by flame-hydrolysis and characterization by TPD-TPR-MS and EPR [J]. Applied Catalysis (B): Environmental, 2000, 28: 55 - 64.

[6]   Rossetti I, Forni L. Catalytic flameless combustion of methane over perovskites prepared by flame-hydrolysis [J]. Applied Catalysis(B): Environmental, 2001, 33: 345 - 352.

[7]   Dai H X, He B H, Li W, et al. Perovskite-type oxide $ACo_{0.8}Bi_{0.2}O_{2.87}$ (A = $La_{0.8}Ba_{0.2}$): a catalyst for low-temperature CO oxidation [J]. Catalysis Letters, 2001, 73(2 - 4): 149 - 156.

[8]   Spinicci R A, Tofanari A A, Faticanti M, et al. Hexane total oxidation on $LaMO_3$(M = Mn, Co, Fe) perovskite-type oxides [J]. Journal of Molecular Catalysis A: Chemical, 2001, 176: 247 - 252.

[9]   Saracco G, Geobaldo F, Baldi G. Methane combustion on Mg-doped $LaMnO_3$ perovskite catalysts [J]. Applied Catalysis (B): Environmental, 1999, 20: 277 - 288.

[10]   DING Tie-zhu, LI Jian, QI Qi-ge, et al. XPS studies on rare earth oxide LSCO/YSZ electrodes [J]. Journal of Rare Earths, 2003, 21(4): 453 - 457. (in Chinese)

[11]   Kowalczyk S P, Ley L, Mcfeely F R, et al. Multiple splitting of the manganese 2p and 3d levels in MnF_2 single crystals [J]. Physics Reviews(B), 1975, 11: 1721.

[12]   LAN Cui-ling, MENG Yan-qiang, ZHAO Lin-yuan, et al. Surface characterization of La-Cu-Mn perovskite-type mixed oxides [J]. Guangxi Sciences, 2002, 9(4): 284 - 288. (in Chinese)

[13]   Rossetti I, Forni L. Catalytic flameless combustion of methane over perovskites prepared by flame-hydrolysis [J]. Applied Catalysis(B): Environmental, 2001, 33: 345 - 352.

[14]   Leanza R, Rossetti I, Fabbrini L, et al. Perovskite catalysts for the catalytic flameless combustion of methane preparation by flame-hydrolysis and characterization by TPD-TPR-MS and EPR [J]. Applied Catalysis (B): Environmental, 2000, 28: 55 - 64.

[15]   PAN Zhi-yong, ZHANG Chang-bin, YU Chang-chun, et al. Study on catalytic combustion of methane over the supported La-Mn perovskite catalysts [J]. Journal of Molecular Catalysis, 2003, 17(4): 274 - 278. (in Chinese)

[16]   LIANG Zhen-cheng, QIN Yong-ning, LIAO Qiao-li, et al. Properties of perovskite-type $La_{1-x}Cu_xMnO_3$ catalysts [J]. Chinese Journal of Applied Chemistry, 1997, 14(1): 11 - 15.

[17]   Fabbrini L, Rossetti I, Forni L. Effect of primer on honeycomb-supported $La_{0.9}Ce_{0.1}CoO_{(3\pm\delta)}$ perovskite for methane catalytic flameless combustion [J]. Applied Catalysis (B): Environmental, 2003, 44: 107 - 116.

(Edited by YANG Bing)